

UNITED STATES  
DEPARTMENT OF THE INTERIOR  
GEOLOGICAL SURVEY

TECHNICAL LETTER NUMBER 4  
CRUSTAL STRUCTURE IN NEVADA AND SOUTHERN  
IDAHO FROM NUCLEAR EXPLOSIONS\*

by

L. C. Pakiser\*\* and D. P. Hill\*\*

DENVER, COLORADO

This page intentionally left blank



UNITED STATES  
DEPARTMENT OF THE INTERIOR  
GEOLOGICAL SURVEY

Technical Letter  
Crustal Studies-4  
October 15, 1962

Dr. Charles C. Bates  
Chief, VELA UNIFORM Branch  
Advanced Research Projects Agency  
Department of Defense  
Pentagon  
Washington 25, D. C.

Dear Dr. Bates:

Transmitted herewith are 10 copies of:

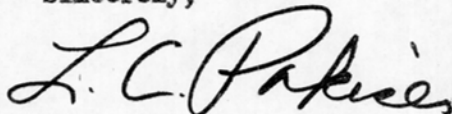
TECHNICAL LETTER NUMBER 4  
CRUSTAL STRUCTURE IN NEVADA AND SOUTHERN  
IDAHO FROM NUCLEAR EXPLOSIONS\*

by

L. C. Pakiser\*\* and D. P. Hill\*\*

We intend to submit this report for publication in a scientific journal.

Sincerely,



L. C. Pakiser, Chief  
Branch of Crustal Studies

\* Work performed under ARPA Order No. 193-62.

\*\* U. S. Geological Survey, Denver, Colorado.

This page intentionally left blank



UNITED STATES  
DEPARTMENT OF THE INTERIOR  
GEOLOGICAL SURVEY

Technical Letter  
Crustal Studies-4  
October 15, 1962

CRUSTAL STRUCTURE IN NEVADA AND SOUTHERN IDAHO  
FROM NUCLEAR EXPLOSIONS\*

by

L. C. Pakiser\*\* and D. P. Hill\*\*

Abstract. The time of first arrival of seismic waves generated by 4 underground nuclear explosions at the Nevada Test Site (NTS) and recorded along a line extending north into southern Idaho is expressed as  $T_0 = 0.00 + \Delta/3.0$  (assumed),  $T_1 = 0.40 + \Delta/6.03$ , and  $T_2 = 6.15 + \Delta/7.84$ , where time is in seconds and the shot-detector distance ( $\Delta$ ) is in km. Assuming constant velocities and horizontal layers, crustal thickness in the vicinity of NTS was determined to be 28 km. Delays in the traveltime segment  $T_2$ , which represents  $P_n$ , indicate that the crust may thicken to 32 km in northern Nevada. A third phase, expressed as  $T_3 = 14.48 + \Delta/7.84$ , was also recognized and has arrival times appropriate for SPS. Amplitudes of  $P_n$  were determined at 7 places from recordings of seismic waves from one underground nuclear explosion (ANTLER).

\* Work performed under ARPA Order No. 193-62.

\*\* U. S. Geological Survey, Denver, Colorado.

UNITED STATES  
DEPARTMENT OF THE INTERIOR  
GEOLOGICAL SURVEY

Technical Letter  
Crustal Studies-4  
October 15, 1962

CRUSTAL STRUCTURE IN NEVADA AND SOUTHERN IDAHO  
FROM NUCLEAR EXPLOSIONS\*

by

L. C. Pakiser\*\* and D. P. Hill\*\*

Introduction. Recordings of seismic waves generated by 4 underground nuclear explosions at the Atomic Energy Commission's Nevada Test Site (NTS) were made by the U. S. Geological Survey at 21 places along a line extending north into the southern part of the Snake River Plain, Idaho (Fig. 1). The nearest recording made was 68.0 km and the most distant one 574.3 km from the source at NTS (Table 1). The remaining 19 recordings were made at places that are spaced approximately uniformly along the line.

The first underground nuclear explosion recorded was ANTLER. ANTLER was detonated at a depth of 1,318 ft in tuff at 17:00:00.17 universal time on September 15, 1961. The yield of ANTLER was 2.4 kt. Information on the date, time, yield, medium, and depth of the remaining 3 explosions has not yet been declassified by the AEC. In each of the recordings after ANTLER, at least one earlier recording location was repeated (Table 1). Only first arrivals, the extension of these first arrivals into the zone of secondary arrivals, and one set of secondary arrivals are presented and interpreted in this paper.

\* Work performed under ARPA Order No. 193-62.

\*\* U. S. Geological Survey, Denver, Colorado.

Figure 1.--Index map showing seismic recording locations with respect to the Nevada Test Site.

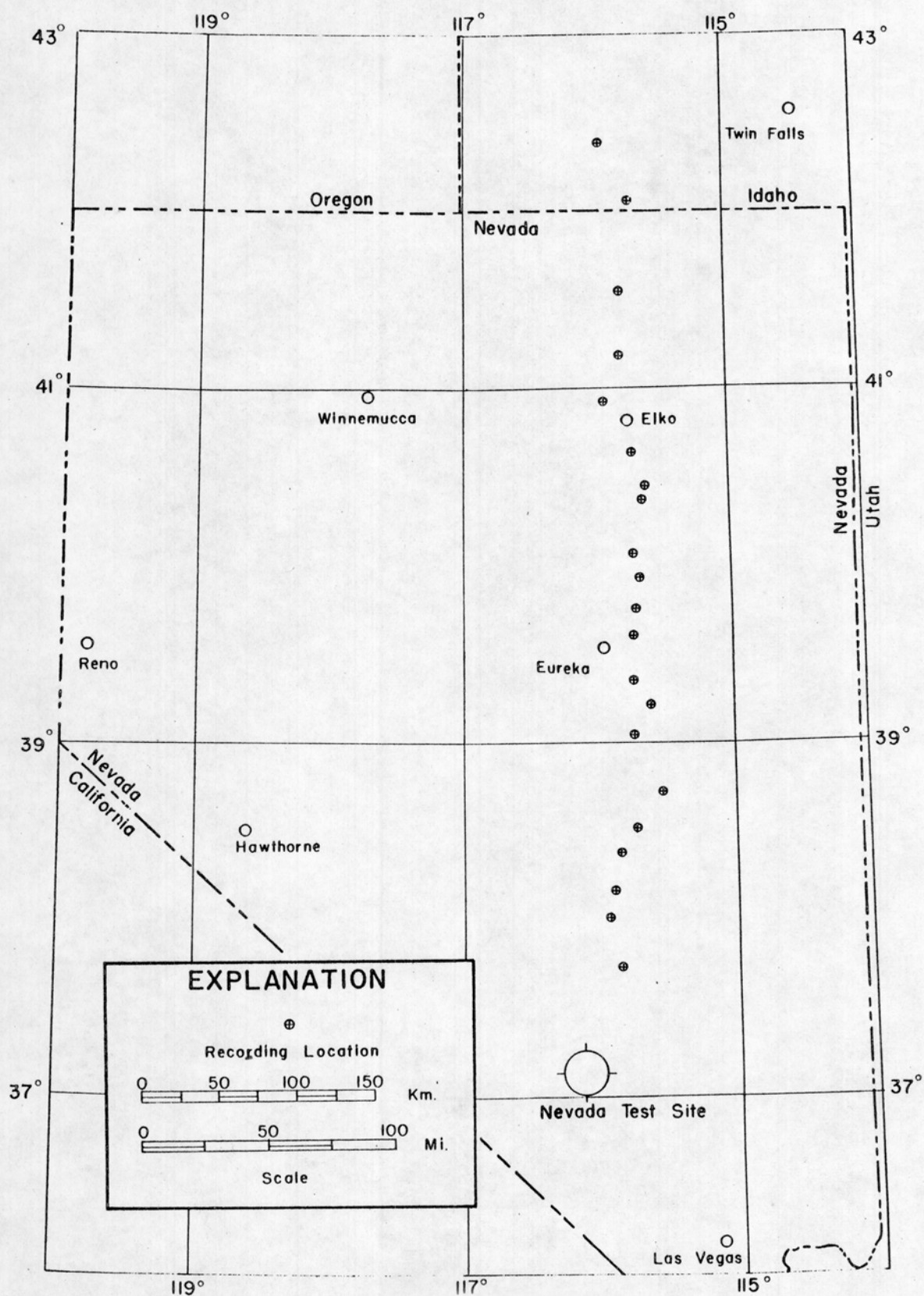




Table 1.--Times of first arrivals and selected secondary arrivals  
with distance and velocities across spreads.

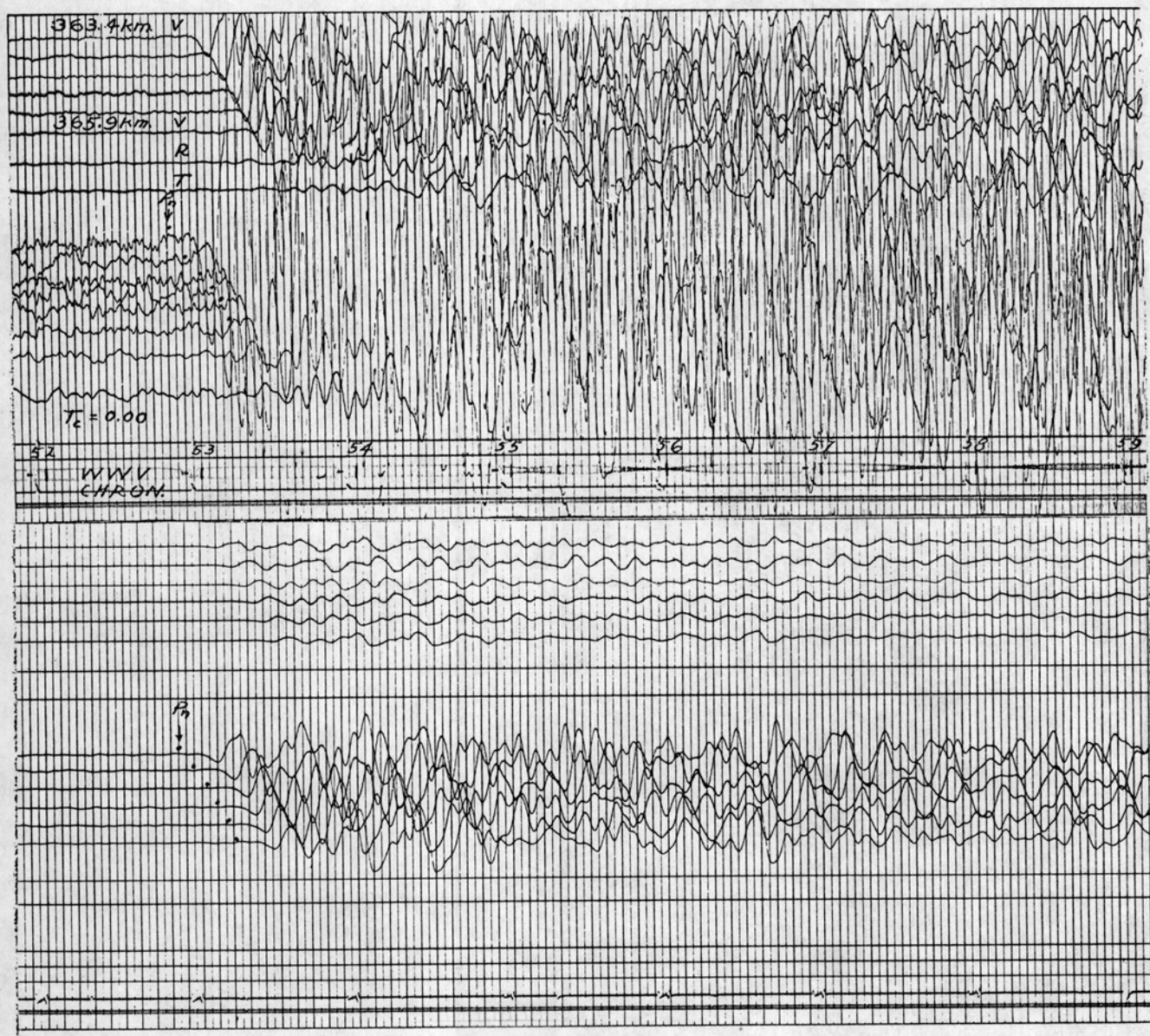
Distance to No. 1 Seismometer, km	Time of first arrival, sec	Velocity across spread, km/sec	Time of secondary arrival, sec	Velocity across spread, km/sec
68.0	11.90	6.0	--	--
98.0	16.65	5.6	18.58	7.1
116.4	20.05	5.4	21.03	5.2
139.1*	24.05	6.8	--	--
139.6*	23.80	5.3	--	--
158.0	26.49	9.3	27.12	5.6
186.5	29.97	6.4	31.54	6.2
205.9*	32.88	7.8	34.65	7.4
210.2*	33.26	7.1	35.54	7.1
215.7*	34.08	6.3	36.35	5.9
235.3	36.60	7.0	39.29	5.9
248.2*	38.56	6.2	41.94	7.5
248.5*	38.55	6.3	41.72	5.2
276.6	42.20	9.0	46.33	10.8
286.2	43.01	8.1	--	--
301.7	44.99	8.3	--	--
327.7	48.28	7.2	56.51	7.6
355.4	51.89	7.4	59.87	5.1
363.4	52.83	6.9	60.92	9.6
381.1	54.79	8.0	63.01	7.4
417.1	59.46	9.3	67.70	8.9
444.5	62.93	10.5	71.11	12.5
485.6	68.22	8.3	76.35	6.8
538.2	74.76	7.0	83.13	10.6
574.3	79.93	8.5		

\*Recording unit at same location; shotpoint moved.

The seismic-refraction instruments used in this study have been described by Warrick and others (1961). The general method of making the recordings has been described by Stewart and Pakiser (in press). The work described in this paper was done on behalf of the Advanced Research Projects Agency, Department of Defense, as a part of VELA UNIFORM under ARPA Order No. 193-62. S. W. Stewart assisted in study of the recordings of ANTLER.

Traveltimes and velocities. Traveltimes of first arrivals were picked to a reading accuracy of 0.01 sec. On some seismograms the first (compressive, up) motion is very clearly defined, and the beginning of the phase can be read to about 0.02 sec. On most seismograms (e.g., Fig. 2) the direction of the first half-cycle can be recognized, but the traveltimes can be read to an accuracy of only about 0.05 or 0.10 sec. On a few seismograms the first compression was obscured by noise, but the first troughs were clearly defined; on such seismograms the time difference between first motion and the first trough was estimated from seismograms recorded at adjacent locations and subtracted from the traveltime of the first trough to yield the traveltime of first motion. The first 3 half-cycles of motion, with one exception, are similar on all recordings. With very few exceptions, all traveltimes (Table 1, Fig. 3) should be reliable to within 0.20 sec. Distances from the source are known to the nearest km or better.

Figure 2.--Seismogram from the ANTILER underground nuclear explosion of September 15, 1961, recorded 363.4-365.9 km from the source, showing  $P_n$  as a first arrival. Upper seismogram is the monitor recorded on photographic paper in the frequency band 1 - 37 cps. Lower seismogram is the magnetic-tape playback recorded in the frequency band 1 - 13 cps. Both seismograms were recorded at two levels of amplification separated by 15 db. Radial and transverse horizontal motion was recorded on the upper seismogram only at the No. 4 vertical seismometer. Vertical motion only was recorded on magnetic tape.





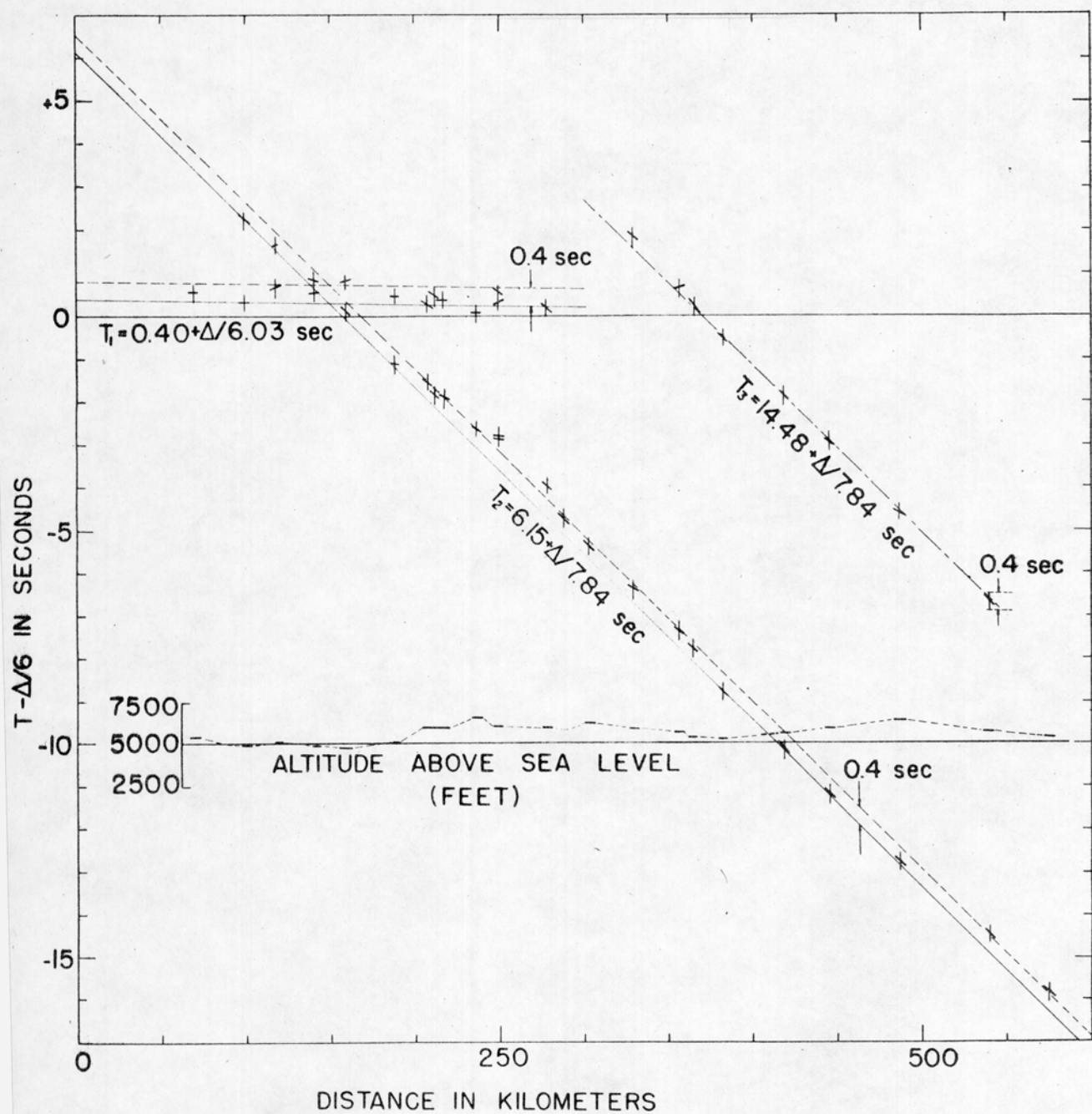


Figure 3.--Reduced traveltime curve for  $T_1$ ,  $T_2$ , and  $T_3$ , representing  $P_g$ ,  $P_n$ , and a wave with traveltimes appropriate for SPS.

Traveltimes from 25 seismograms of first and selected secondary arrivals were tabulated (Table 1) and plotted in the reduced form  $T - \Delta/6$  sec as a function of  $\Delta$  km (Fig. 3). No corrections for elevation or near-surface velocity differences at either sources or recording locations were made. The recordings at 139.1 and 139.6; 205.9, 210.2, and 215.7; and 248.2 and 248.5 km (Table 1) were made at the same locations but the sources at NTS were in different places. Maximum deviations from the 6.03 km/sec and 7.84 km/sec traveltime segments (Fig. 3) for these repeated recordings are 0.3, 0.2, and 0.1 sec respectively. Presumably these deviations represent the combined effect of variations in the near-surface velocity and elevation at the sources, and timing errors. However, the shots for which initial and repeated recordings were made near 139 and 248 km were the same, and the deviations should be the same. The first motion was probably not detected at 139.1 km, so the traveltime given is assumed to be that of a secondary arrival along the 7.84 km/sec traveltime segment rather than a first arrival along the 6.03 km/sec segment. This conclusion is supported by the different velocities across the spread at 139.1 and 139.6 km, which are 6.8 and 5.3 km/sec respectively (Table 1). The 6.03 and 7.84 km/sec arrivals are almost simultaneous at this location. The velocities across the spread at 248.2 and 248.5 km are virtually the same (Table 1).

Lines representing seismic waves traveling at 6.03 and 7.84 km/sec respectively were drawn through the earliest first and secondary arrivals along these traveltime segments (Fig. 3). These lines were drawn

through the earliest arrivals to eliminate as much as possible the effects of changes in the velocity and thickness of the near-surface low-velocity zone along the line. Parallel lines 0.4 sec later were also plotted. With few exceptions, all arrivals lie within this 0.4-sec interval. The 6.03 km/sec traveltime segment, the  $P_g$  phase of seismology, is expressed by:

$$T_1 = 0.40 \pm 0.20 + \Delta/6.03 \pm 0.10 \text{ sec}$$

and the 7.84 km/sec segment,  $P_n$ , by:

$$T_2 = 6.15 \pm 0.20 + \Delta/7.84 \pm 0.10 \text{ sec.}$$

A third phase with the velocity of  $P_n$  but arriving 8.33 sec later was also identified. This phase has arrival times appropriate for SPS and is expressed by:

$$T_3 = 14.48 \pm 0.20 + \Delta/7.84 \pm 0.10 \text{ sec.}$$

The velocity across the spread for each of the first and secondary arrivals was calculated from the spread length projected on a line to the source and the time difference between the first and last seismometer of each spread (Table 1). The spreads were 2-1/2 km long, and the projection of most spreads (oriented in general north) along a line to the source was slightly less than 2-1/2 km. The velocity across each spread was also plotted on the reduced traveltime curve, but the lengths of these segments were exaggerated for clarity (Fig. 3). The spread or interval velocity for  $P_g$ , in the range where it is a first arrival, is 5.3 to 6.8 km/sec, and the average is 5.82 km/sec. This compares favorably with 6.03 km/sec from the traveltime curve. However, as mentioned previously, the 6.8 km/sec interval velocity may represent



a secondary arrival. The interval velocity for  $P_n$  where it is represented by first arrivals lies in the range 6.2 to 10.5 km/sec, and the average is 7.74 km/sec, compared with 7.84 km/sec from the traveltime curve. Therefore, interval velocity, despite the wide scatter, is a useful criterion for phase recognition.

Traveltimes and crustal structure. Using the traveltime segments  $T_1$  and  $T_2$  from the previous section and the assumed relation  $T_0 = 0.00 + \Delta/3.0$  sec for the near-surface materials, a model representing the average crust in east-central Nevada was computed (Table 2). This is a one-layer crust with a near-surface low-velocity zone that can be deduced directly from first arrivals. The probability of a layer of intermediate velocity in the lower part of the crust will be discussed in a later section.

Table 2.--Crustal model in east-central Nevada

Layer	Compressional-wave velocity, km/sec	Layer thickness, km	Depth to bottom of layer, km
0	3.0 (assumed)	0.7	0.7
1	6.03 ( $P_g$ )	27.0	28*
2	7.84 ( $P_n$ )	--	--
* Rounded to nearest km.			

Uncertainties concerning the near-surface velocities at the various shot locations, and a lack of knowledge of the near-surface velocities at recording locations, make meaningless any attempt to include a refined

interpretation of the velocity distribution near the surface. The assumed velocity of 3.0 km/sec is intended to be a generalized average of the velocities of all materials, including alluvium, tuff, and the upper part of the pre-Tertiary rocks, that cause the intercept of 0.4 sec in the 6.03 km/sec traveltime segment. The effect on crustal thickness of varying the velocity of the near-surface low-velocity zone through a range of reasonable values in making computations is not very great.

$P_n$  arrivals in the distance range 180 to 380 km from NTS are delayed with respect to the 7.84 km/sec traveltime segment (Fig. 3). Only two of these arrivals are delayed by more than 0.4 sec, however, and these larger delays may be the result either of failure accurately to detect first motion or of larger than average thicknesses of near-surface low-velocity materials. Ignoring these two late arrivals and attributing all of the 0.4 sec delay to an increase in crustal thickness requires increasing the depth to the crust-mantle interface by 4 km to 32 km. This area of thicker crust would be in the high Basin Ranges of Nevada between, roughly, Eureka and Elko (Figs. 1 and 3).

The possibility was also considered that the delay could be the result of crustal velocities substantially less than 6.03 km/sec or to a greater accumulation of low-velocity materials near the surface. An attempt was made to correlate  $P_n$  delays with thick accumulations of alluvium in the valleys between high ranges, but no obvious relation between the two was found. J. P. Eaton (written communication), in

interpreting a seismic-refraction profile between Eureka and Fallon, Nevada, found a  $P_g$  velocity of 6.02 km/sec. This is virtually identical to the  $P_g$  velocity of 6.03 km/sec found in this study. Eaton's intercept time for  $P_g$  is 0.7 sec, and this larger intercept could account for part of the 0.4-sec delay. However, Eaton was interpreting seismograms from relatively small chemical explosions, so it is possible that he was reading a somewhat later time for  $P_g$  than the earliest first motion from underground nuclear explosions interpreted in this paper. Finally, the computed thickness of a one-layer crust of 32 km in the vicinity of Eureka compares identically with a thickness of 32 km determined by Eaton in interpreting the reversed profile from Eureka to Fallon.

It seems likely, therefore, that the crust is actually thicker in the region of these delays.

The 0.4-sec delay of  $P_n$  at the most distant two recording locations could be caused by a thickening of the crust under the southern part of the Snake River Plain (Figs. 1 and 3). First arrivals were weak, however, on seismograms made at these two places, so it is likely that the delay is the result of failure to detect first motion.

Comparison with earlier investigators. Diment, Stewart, and Roller (1961) presented a comparison of their results with those of previous investigators. For ready reference and comparison with our new data, the results of earlier investigators of crustal structure in the Basin and Range Province are recapitulated here (Table 3).



Table 3.--Summary of crustal structure  
in the Basin and Range Province

Investigators	Velocity of $P_g$ , km/sec	Velocity of $P_n$ , km/sec	Crustal thickness, km
Tatel and Tuve (1955)	5.5	8	29
Press (1960)	6.11	7.66*	24
Berg, Cook, Narans, and Dolan (1960)	5.73, 6.33	7.59*	25
Diment, Stewart, and Roller (1961)	6.15	7.81*	28
Pakiser and Hill	6.03	7.84	28
* Not identified as $P_n$ in reference.			

The consistency of most of these results is impressive, especially when it is recalled that the results of these earlier investigators were based on measurements with the relatively crude instruments available to them at the time and energy sources that were often not well suited to refraction profiling. Tatel and Tuve (1955) recorded seismic waves generated by blasts at Bingham Canyon, Utah, near the eastern margin of the Basin and Range province, so their results may not be directly comparable with ours. The same may be said of the results of Press (1960), who studied an average crust between Corona, California, and NTS, only part of which is within the Basin and Range Province. The results of Berg and others (1960) were based on recordings in northern Utah and northeastern Nevada of seismic waves generated by blasts at Promontory and Lakeside, Utah, and therefore include data in the area of this study.

Diment, Stewart, and Roller (1961) studied the area southeast of NTS to Kingman, Arizona, an area wholly within the Basin and Range Province. Their results are almost identical to ours. However, a recent reversal of the NTS-Kingman profile from a shotpoint near Kingman indicates that the crust-mantle interface dips up from NTS to Kingman to a depth of 26 km at Kingman and that the true velocity of  $P_n$  along the profile is 7.7 km/sec (J. C. Roller, written communication). Therefore the crust may thicken from 26 km near Kingman to 32 km in northern Nevada.

Press (1960) identified the 7.66 km/sec layer as an intermediate crustal layer, and found evidence for a layer with a velocity of 8.11 km/sec at a depth of 50 km. No evidence was found for this layer in the present study, nor for the layer with a velocity of 7.97 km/sec at a depth of 72 km reported by Berg, Cook, and Narans (1960). Press (1960), Berg and others (1960), and Diment, Stewart, and Roller (1961) did not identify the layer with velocity in the range 7.59 to 7.81 km/sec as  $P_n$ , nor the depth to this layer as crustal thickness. The upper surface of this layer, which we associate with our layer with a velocity of 7.84 km/sec, is the most prominent velocity boundary in the Basin and Range Province and should be taken to represent the Mohorovicic discontinuity or crust-mantle interface. The low velocities of 7.66 km/sec and 7.59 km/sec reported by Press (1960) and Berg and others (1960) for this layer may be apparent downdip velocities or the results of scatter in the data they interpreted.

Intermediate crustal layer. No evidence was found for a layer of intermediate velocity in the lower part of the crust from the first arrivals interpreted in this paper. Some suggestions of secondary arrivals that could be interpreted as refractions or reflections from such a layer were found, but these secondary arrivals were not sufficiently consistent among themselves to justify drawing traveltime segments on the reduced traveltime curve (Fig. 3).

Eaton (written communication) found 2 strong phases on seismograms recorded west of a shotpoint at Eureka which he interpreted as reflections from an intermediate layer and from the Mohorovicic discontinuity. The depth to this intermediate layer of velocity about 6.7 km/sec would be 23 km at Eureka, requiring the depth to the crust-mantle interface to be increased to 36 km.

Clear evidence for an intermediate layer of velocity 6.7 km/sec was found from first arrivals along reversed profiles extending north from Elko to near Boise, Idaho. A final interpretation of these profiles, as well as additional recordings of seismic waves from underground nuclear explosions at NTS, is in progress. The preliminary depth to the intermediate layer at Elko is 15 km, and this layer rises to within about 10 km of the surface at the northernmost limit of the profile interpreted in this paper.

If this intermediate layer is present throughout the profile from Kingman to southern Idaho, it would require that crustal thicknesses be increased to about 28 km at Kingman, 31 km at NTS, and 36 km between Eureka and Elko.



Amplitudes of P. Amplitudes of the first peak-to-peak motion of seismic waves generated by ANTILER were determined at seven locations in the range 210.2 to 485.6 km from the source (Fig. 4, Table 4). The peak-to-peak amplitude S (Fig. 4) was measured in microvolts and converted to millimicrons of ground displacement ( $1/2$  peak to peak) from the calibration constants of the instruments and the frequency as estimated from the first half period  $1/2 T$  (Fig. 4). The method of computing ground displacement was derived by Eaton (written communication).

Except for the amplitude at 210.2 km, amplitudes fall off with distance, but with considerable scatter. The curve representing inverse-cube attenuation with distance is presented for reference only (Fig. 4). Amplitudes of the first motion from ANTILER are about  $1/6$  those reported by Romney (1959) for BLANCA and LOGAN, scaled down to the yield of ANTILER (2.4 kt). But Romney determined the maximum amplitude of the first few cycles of motion following  $P_n$ . The maximum amplitudes of the first few cycles of motion following  $P_n$  on seismograms interpreted in this study are about 6 times those determined from measurements of S, so these amplitudes are in general agreement with those of Romney.

The very low amplitude at 210.2 km was measured for a wave of frequency significantly less than that of the remaining recordings (Table 4). The lower amplitude and frequency may be the result of attenuation of the higher frequencies by near-surface effects such as a larger than average accumulation of low-velocity alluvium or complexities in the geologic structure in the immediate vicinity of the recording location.

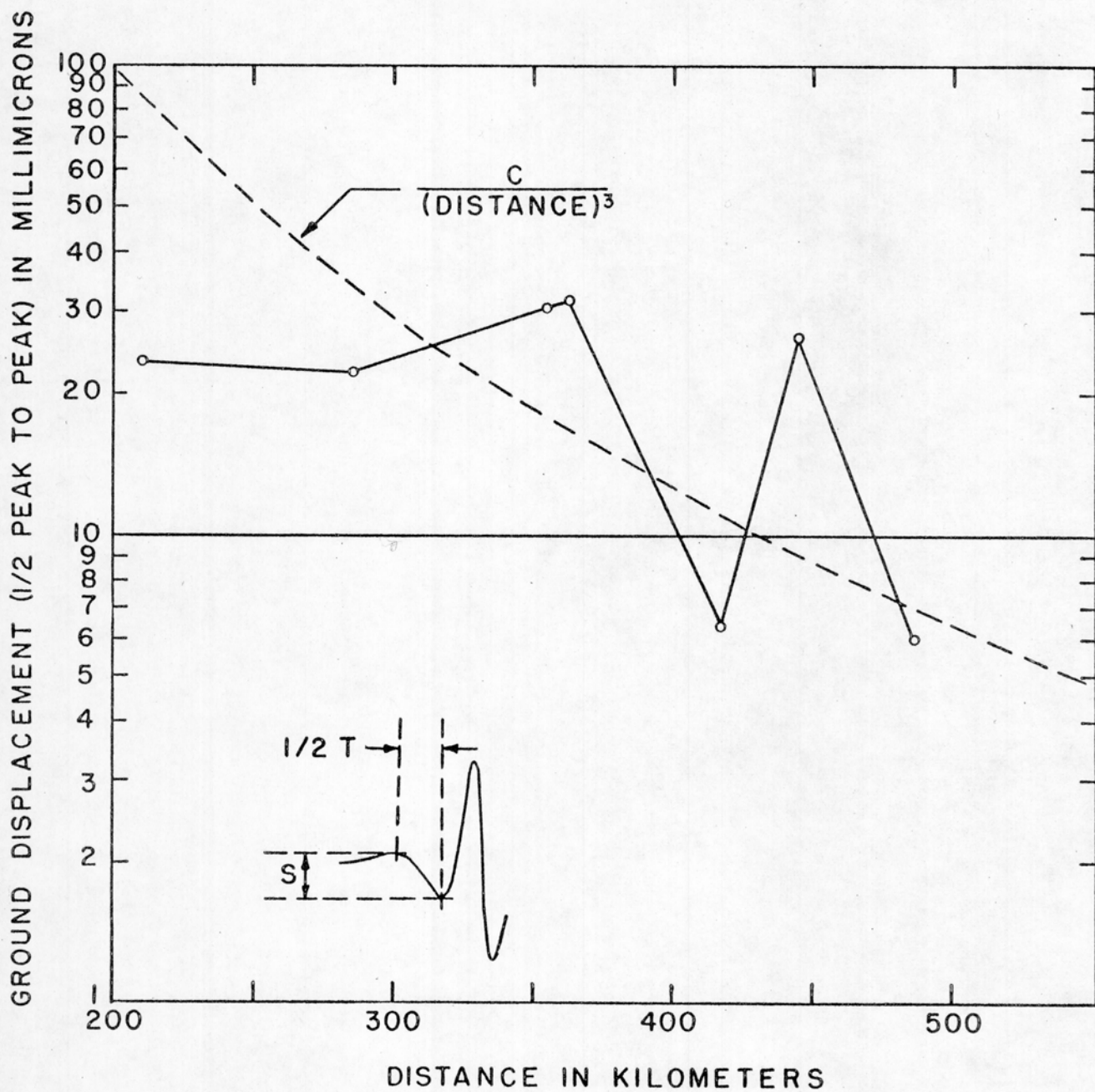


Figure 4.--Amplitudes of first motion from ANTLEP.

Table 4.--Amplitudes and frequencies  
of first motion with distance

Distance to No. 1 Seismometer, km	Frequency cps	Amplitude of 1st Motion, 1/2 peak to peak, in millimicrons
210.2	2.6	23.4
286.2	4.1	22.2
355.4	4.0	30.4
363.4	3.7	31.7
417.1	5.2	6.4
444.5	4.3	26.5
485.6	4.5	6.0*
*Evidence of interference during first 1/2 cycle of first motion.		



The phase  $T_3$ . The phase of traveltimes  $T_3$  (Fig. 3) was recorded as an identifiable phase at all distances between 327.7 and 538.2 km from the source. It is probably present at both smaller and larger distances, but at these distances it is lost in a train of waves that begin earlier and persist for several seconds. In this study it was picked on the seismograms, plotted on the reduced traveltime curve, and correlated from recording location to recording location. It was first recognized from vertical motion only as a phase that follows  $P_n$  by 8.33 sec with the velocity of  $P_n$ . Re-examination of the seismograms revealed that amplitudes of horizontal motion increase with the arrival of this phase, but the particle motion is complex and not appropriate for either pure SV or P motion.

The phase  $T_3$  has evidently traveled along the Mohorovicic discontinuity as a P wave, and the delay from  $P_n$  might be accounted for by any of the following paths if the traveltimes are appropriate: PPS, SPP, and SPS, which follow refraction paths and involve P to S or S to P conversions, or PPPPP and PPPPS, which involve multiple crustal paths and reflection from the surface. Of these paths, only SPS has unambiguous traveltimes for any crust except one of constant thickness.

To test these paths, a crustal shear velocity of 3.50 km/sec and a near-surface shear velocity of 1.74 km/sec were assumed, and computations were made of hypothetical intercept times. The 3.50 km/sec shear velocity is essentially the same as the 3.49 km/sec determined by Press (1960) for  $L_g$ . The  $S_g$  phase on seismograms interpreted in this paper was not

sufficiently sharp for determination of velocity. The value of  $S_g$  determined from observations is 3.53 km/sec, but this gave too large an intercept time.

Intercept times for the various paths would be as follows:  
PPS and SPP, 10.36 sec; SPS, 14.56 sec; PPPPP, 12.30 sec: and PPPPS, 16.51 sec. Of these, the computed intercept time for SPS of 14.56 sec is nearly identical to the measured intercept time for  $T_3$  of 14.48 sec. None of the other intercept times are within 2 sec of the measured intercept time. Therefore, although the particle motions of the  $T_3$  arrivals are not appropriate for SV, the traveltimes provide evidence that the phase may be SPS, perhaps involving interference from a mixture of compressional and shear waves that have traveled many paths that involve complex P to S and S to P conversions at several boundaries along the downward and emergent paths.

The association of the phase  $T_3$  with SPS is provisional and cannot be presented confidently without additional research on SPS and other possible phases that we would expect to be recorded on seismograms.

If SPS can be identified on seismograms, its path has geometric properties that can be extremely useful. For example:

1. If the velocity structure of the crust and crust-mantle interface is known, the time interval between SPS and  $P_n$  can be used to determine focal depths.

2. The apparent velocities of SPS and  $P_n$  can be used to compute the dip, the true velocity of compressional waves in the upper-mantle rocks, and variations in crustal thickness from an unreversed profile.

3. If crustal structure is known at a source of known focal depth, it can be determined at a remote seismic-refraction line from the SPS- $P_n$  time interval and assumed of known shear- and compressional-wave velocities in the crust and the compressional-wave velocity in the upper-mantle rocks.

(Relations for determination of these quantities are given in Appendix A and Appendix B.)

The potential power of SPS in determination of focal depths and crustal structure suggests further experimental and theoretical research on this and other phases involving P to S or S to P conversions and multiple crustal paths.



## APPENDIX A

Computation of focal depth from SPS. The vertical distance  $h$  between the source and the crust-mantle interface (Fig. 5) is given by:

$$h = (T_{S-P} - C) / k \quad h_0 < f,$$

where:

$T_{S-P}$  is the time difference between SPS and  $P_n$ ,

$$C = h_1 (\cos \beta_s / V_1 - \cos \beta_p / v_1) + h_0 (\cos \alpha_s / V_0 - \cos \alpha_p / v_0),$$

$$k = \cos \beta_s / V_1 - \cos \beta_p / v_1,$$

$$\sin \alpha_s = V_0 / v_2,$$

$$\sin \alpha_p = v_0 / v_2,$$

$$\sin \beta_s = V_1 / v_2, \text{ and}$$

$$\sin \beta_p = v_1 / v_2.$$

$V_0$ ,  $v_0$ ,  $V_1$ , and  $v_1$  are the shear- and compressional-wave velocities in layers 0 and 1, respectively, and  $v_2$  is the compressional-wave velocity in layer 2.

Then  $f = D_1 - h$ , where  $D_1 = h_1 + h_0$  (Fig. 5).

For the crustal model of this study (accepting  $T_3$  as defining the traveltimes of SPS),  $C$  was computed as 4.22 and  $k$  as 0.150. However,  $C$  is simply one-half the time difference between SPS and  $P_n$  for zero focal depth, or 4.17 as taken from the reduced traveltime curve (Fig. 3).

Crustal thickness,  $D_1$ , is 28 km.

As a test of this method of determining focal depths, the calibration constants of the crust,  $C$ ,  $D_1$ , and  $k$  were determined from traveltimes for ANTILER, and focal depths for two later explosions were computed from the time interval between  $T_3$  and  $P_n$ . Both focal depths were less than 1 km. The restriction that  $f$  be greater than  $h_0$  was ignored in making these computations.

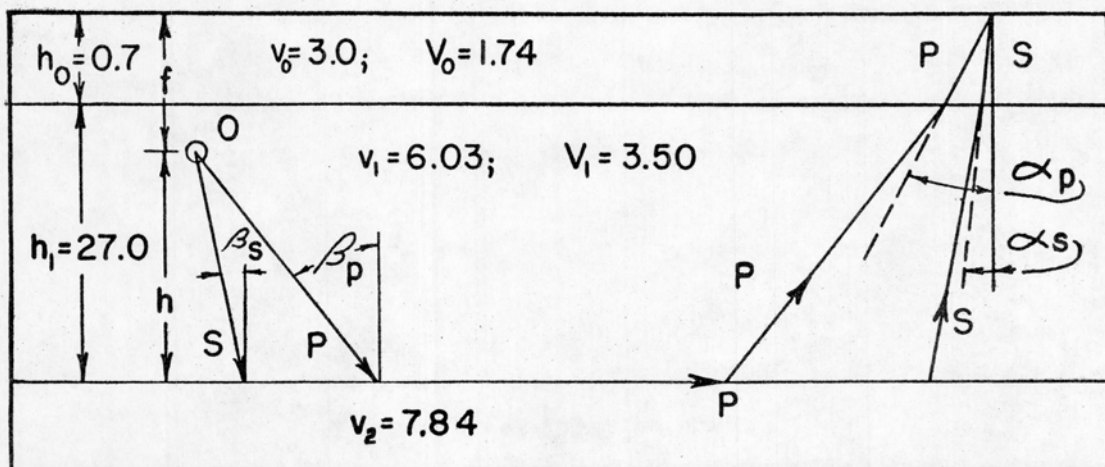


Figure 5.--Geometric relations for determination of focal depth from SPS and  $P_n$ .

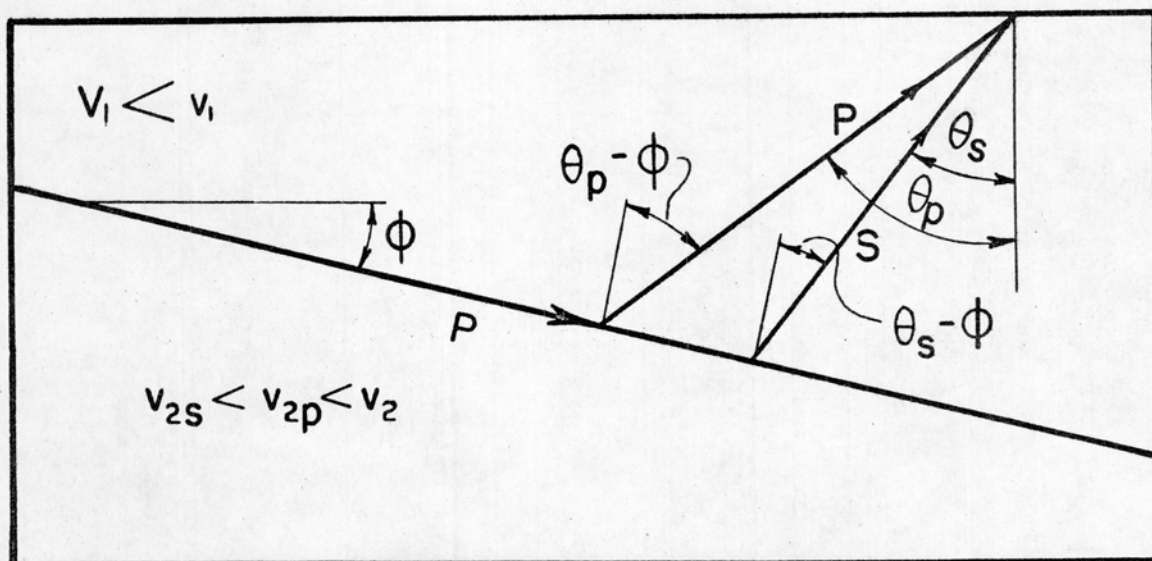


Figure 6.--Geometric relations for determination of dip and true velocity of compressional waves in the upper mantle rocks from SPS and  $P_n$ .

## APPENDIX B

Crustal structure from SPS. We are indebted to J. H. Healy for suggesting the simple solution for dip  $\varphi$  and true velocity of compressional waves in the upper-mantle rocks  $v_2$  that follows (Fig. 6). For the downdip case, in which  $V_1$  is the velocity of shear waves in the crust,  $v_1$  is the velocity of compressional waves in the crust, and  $v_{2S}$  and  $v_{2P}$  are the apparent velocities of SPS and  $P_n$ :

$$\sin \theta_p = v_1/v_{2P},$$

$$\sin \theta_s = v_1/v_{2S},$$

$$\sin (\theta_p - \varphi) = v_1/v_2,$$

$$\sin (\theta_s - \varphi) = v_1/v_2,$$

$$\sin \theta_p \cos \varphi - \cos \theta_p \sin \varphi = v_1/v_2,$$

$$\sin \theta_s \cos \varphi - \cos \theta_s \sin \varphi = v_1/v_2.$$

By eliminating  $v_2$  between the two simultaneous equations above:

$$\tan \varphi = (\sin \theta_s/v_1 - \sin \theta_p/v_1) / (\cos \theta_s/v_1 - \cos \theta_p/v_1)$$

or, in terms of velocities:

$$\tan \varphi = V_1 v_1 (v_{2P} - v_{2S}) / (v_1 v_{2P} \sqrt{v_{2S}^2 - v_1^2} - v_1 v_{2S} \sqrt{v_{2P}^2 - v_1^2}).$$

Similarly, for the updip case:

$$\tan \varphi = V_1 v_1 (v_{2P} - v_{2S}) / (v_1 v_{2S} \sqrt{v_{2P}^2 - v_1^2} - v_1 v_{2P} \sqrt{v_{2S}^2 - v_1^2}).$$

The true velocity of compressional waves in the upper-mantle rocks can be determined from the relations:

$$v_2 = v_1 / \sin (\theta_p - \varphi) = v_1 / \sin (\theta_s - \varphi).$$

Crustal thickness can then be determined from a geometric consideration of the paths for SPS and  $P_n$ , using intercept-time or cross-over distance formulas for the two phases.



The expression for  $h$  as a function of  $T_{s-p}$ ,  $C$ , and  $k$  can be used to compute crustal thickness at a remote seismic-refraction line where  $C$  is determined for a source of known focal depth at a place where the crustal thickness, crustal shear- and compressional-wave velocities, and compressional-wave velocities in the upper mantle rocks are known, and  $k$  is determined for the area in which the recordings are made.

#### REFERENCES

- Berg, J. W., Jr., K. L. Cook, H. D. Narans, and W. M. Dolan, Seismic investigation of crustal structure in the eastern part of the Basin and Range Province: Bull. Seism. Soc. Am., 50, 511-536, 1960.
- Diment, W. H., S. W. Stewart, and J. C. Roller, Crustal structure from the Nevada Test Site to Kingman, Arizona, from seismic and gravity observations: J. Geophys. Research, 66, 201-214, 1961.
- Press, F., Crustal structure in the California-Nevada region: J. Geophys. Res., 65, 1039-1051, 1960.
- Romney, C., Amplitudes of seismic body waves from underground nuclear explosions: J. Geophys. Res., 65, 1809-1814, 1960.
- Stewart, S. W., and L. C. Pakiser, Crustal structure in eastern New Mexico interpreted from the GNOME explosion: Bull. Seism. Soc. Am., (in press).
- Tatel, H. E., and M. A. Tuve, Seismic exploration of a continental crust, Geol. Soc. Am. Spec. Paper 62, 35-50, 1955.
- Warrick, R. E., D. B. Hoover, W. H. Jackson, L. C. Pakiser, and J. C. Roller, The specification and testing of a seismic-refraction system for crustal studies: Geophysics, 26, 820-824, 1961.